

## REYNOLDS NUMBER EFFECT ON THE TRANSITION ON A FLAT PLATE

Antoš P.\* and Jonáš P.

\*Author for correspondence

Institute of Thermomechanics, Academy of Sciences of the Czech Republic,  
 Dolejšková 5, 182 00 Prague, Czech Republic,

Europe,

E-mail: [antos@it.cas.cz](mailto:antos@it.cas.cz)

### ABSTRACT

There are presented some fundamental boundary layer characteristics of the flat plate boundary layer transitional region when changing the flow velocity and the external turbulence level. Experiments were performed in the new experimental set up of the close circuit wind tunnel IT AS CR. The investigated boundary layers are developing on the flat plate in the channel with constant cross section 0.9 m x 0.5 m. The external flow Reynolds number control was executed by velocity variation from about 5 m/s up to 14 m/s. Dimensionless mean flow characteristics and location of the flat plate boundary layer transitional region were investigated.

### INTRODUCTION

The experiments were carried out in the closed type wind tunnel and the investigated boundary layers were developing on smooth flat plate. In fig. 1, the scheme of the wind tunnel setup is shown and orthogonal coordinate system is introduced.

The wind tunnel has a cross section of 0.9 m x 0.5 m. The length of a flat plate was of 2.65 m. The flat plate was made of laminated wood board and the surface was aerodynamically smooth.

### NOMENCLATURE

$x, y$	[m]	Cartesian coordinates
$u, v$	[m/s]	fluctuations of fluid velocity in direction $x, y$
$U_e$	[m/s]	free-stream velocity
$x_G$	[m]	distance of the grid upstream of the leading edge
$Iu_e$	[-]	free-stream intensity of turbulence
$\tau_w$	[Pa]	wall shear stress
$\delta_{99}$	[m]	customary boundary layer thickness
$\delta_1$	[m]	displacement thickness
$\delta_2$	[m]	momentum thickness
$H_{12}$	[-]	shape factor
$Re_2$	[-]	Reynolds number based on a momentum thickness
$C_f$	[-]	skin friction coefficient
$C_{fBI}$	[-]	skin friction coefficient from the Blasius solution
$C_{fLT}$	[-]	Ludwig and Tilmann skin friction coefficient

To the flat plate was attached a MSE6 leading edge. This type of leading edge, described by Schrader at al. [4], has a shape defined by

$$\left(\frac{y}{b}\right)^2 = 1 - \left(\frac{a-x}{a}\right)^p ; \quad p = 2 + \left(\frac{x}{a}\right)^2 \quad (1)$$

and aspect ratio was set to  $a/b=6$ ,  $a=0.036$  m. In previous experiments, it was also used a thin leading edge K1 (radius 1 mm, thickness 2 mm, for description see [1]).

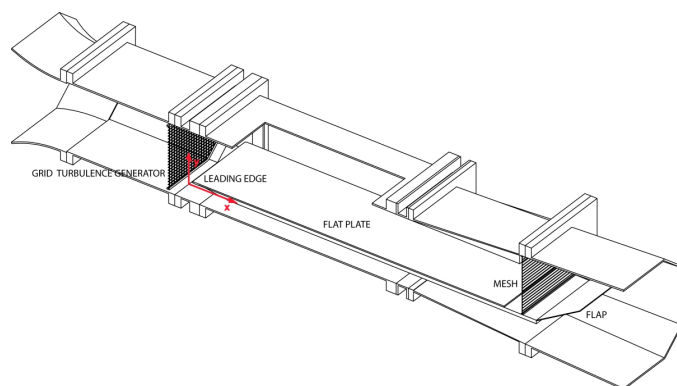


**Figure 1** Experimental setup of the flat plate – coordinate system

The circulation around the plate is compensated by means of deflected flap and a mesh across the flow placed downstream the test section. An adjustable upper wall of test section allows set fine diffuser/confuser channel. Due to all this means and fine adjusting of the angle of attack of the plate, the free stream velocity is kept constant along the test section of the plate ( $U_e(x=0) = U_e(x=1.65$  m) within the limits of measurement accuracy  $\pm 0.5\%$ , farther downstream slowly decreases to  $U_e(x=2.40$  m) =  $0.96U_e(x=0)$ ).

The free stream turbulence was either natural or amplified by the grid upstream from the plate's leading edge. The external flow has the natural turbulence level  $Iu_e=0,3\%$ . The

grid generator of turbulence has a square mesh (rod diameter of 1.65 mm, mesh length of 5.75 mm). Being placed at  $x_G=0.194$  m, it gives turbulence intensity  $Iu_e = 3\%$  at the leading edge. The CTA measurements in free stream show that grid generates homogenous and close to isotropy turbulence.

## MEASUREMENT TECHNIQUE

The mean flow characteristics were measured by a Prandtl tube at the inlet of test section. Measurement of the skin friction was carried out using a coupled pressure probe traversed over the surface or a multiple Pitot rake. A hot-wire X-probe or a single wire probe were used for measurement of the free stream turbulence characteristics or intermittency respectively. The measurement was performed by CTA system - Dantec Streamline.

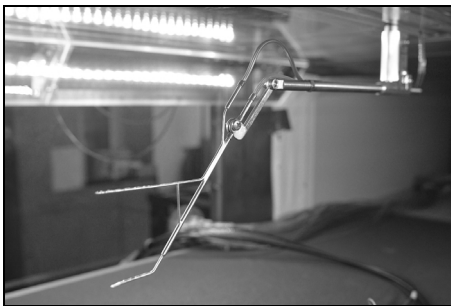


**Figure 2** The coupled pressure probe and traversing system

The coupled pressure probe (see fig. 2) is used for the local dynamic pressure measurement. It consists of a flattened Pitot probe (0.18 mm x 2.95 mm) and a round nosed static pressure probe (dia 1.8 mm). It is connected to pressure transducer Baratron (range 1 kPa, accuracy  $\pm 0.02\%$  of reading value above 20 Pa). The probe was put into defined positions by the traversing system. The distance  $y$  from the wall is measured by cathetometer with accuracy  $\pm 0.02$  mm.



**Figure 3** The multiple Pitot rake

For the velocity-profile measurement of boundary layer was employed the multiple Pitot rake (see fig. 3) scanned by Pneumatic intelligent pressure scanner 9010 - Pressure Systems (16 pressure inputs, range 2.5 kPa, measurement resolution  $\pm 0.003\%$  FS, static accuracy  $\pm 0.15\%$  FS). The multiple Pitot rake was redesigned and manufactured to obtain the velocity profile of boundary layer at once. It significantly speeded up the preliminary experiments.

The reference value of the free stream velocity is measured by Prandtl probe (dia 6 mm) connected to pressure transducer

Druck DPI 145 (range 7 kPa, accuracy  $\pm 0.005\%$  FS). Barometric pressure is measured also by Druck DPI 145. The differential pressure between the barometric and the local static pressure was measured by pressure transducers Omega PX653-0.5D5V (range 125 Pa, repeatability 0.05% FS).

The flow temperature was measured by thermometer Pt100. Output voltage from the transducers were read by Data acquisition unit HP 34970A. Measurement averaging time was set to 20 s. In case of HW measurement there were recorded 30 s time series (frequency 75 kHz, 2.25e6 samples, 16 bit).

## MEASUREMENT UNCERTAINTIES

The experimental uncertainties are estimated based on calculated root mean square errors of interpolations and observed repeatability. The upper limits of relative errors of evaluated quantities depends mainly on accuracy of dynamic pressure measurement: reference dynamic pressure  $\Delta q_r/q_r = \pm 0.02$  ( $U_e = 5$  m/s), local dynamic pressure  $\Delta q/q = \pm 0.02$  ( $U(x,y) > 0.6$  m/s),  $\Delta p = \pm 5$  Pa,  $\Delta U = \pm 0.1$  m/s,  $\Delta \delta_1/\delta_1 = \Delta \delta_2/\delta_2 = \pm 0.015$ ,  $\Delta H_{12}/H_{12} = \pm 0.03$ . The estimated accuracy of evaluation of skin friction  $\tau_w$  is about 4% using coupled pressure probe or up to 8% using multiple Pitot rake.

## RESULTS

The main characteristics evaluated from measurement are: the customary boundary layer thickness  $\delta_{99} = \gamma(U = 0.99U_e)$ , the displacement thickness  $\delta_1$ , the momentum thickness  $\delta_2$ , the wall shear stress  $\tau_w$ , the shape factor  $H_{12}$ , and the skin friction coefficient  $C_f$ .

Boundary conditions of investigated boundary layers are given in the following table.

B.L. No.	$U_e$ (m/s)	$Iu_e$ (%)	L.E.	Reference
1	5	0.3	MSE6	
2	10	0.3	MSE6	
3	14	0.3	MSE6	
4	5	3.0	MSE6	
5	10	3.0	MSE6	
6	14	3.0	MSE6	
13	5	3.0	K1	[1]
14	5	0.3	K1	[2]
15	5	3.0	K1	[2]

**Table 1** Investigated boundary layers

The graph in fig. 4 shows the skin friction coefficient vs. the momentum Reynolds number. One can see that in case of natural turbulence the skin friction coefficient  $C_f$  (1) starts its transitional increase at lower values of  $Re_2$  then  $C_f$  (14). Similarly, in case of grid turbulence, the increase of the skin friction coefficient  $C_f$  (4) starts at lower  $Re_2$  then  $C_f$  (13). It corresponds with the shape factor  $H_{12}$ , shown in fig. 5.

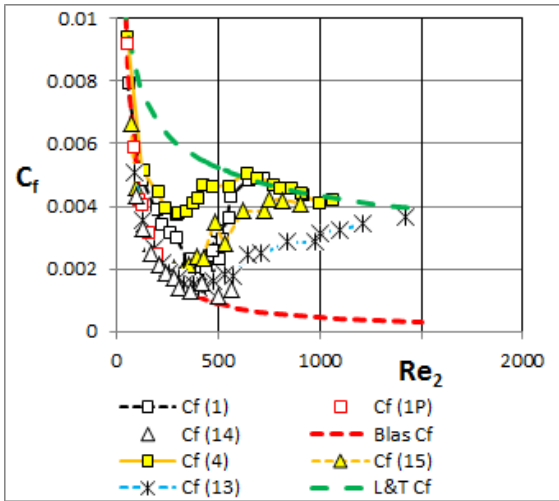


**Figure 4** The skin friction coefficient  $C_f=f(Re_2)$ ;  $U_e=5$  m/s; B.L.: (1,4,13,14,15),  $C_{fBl}$ ,  $C_{fLT}$

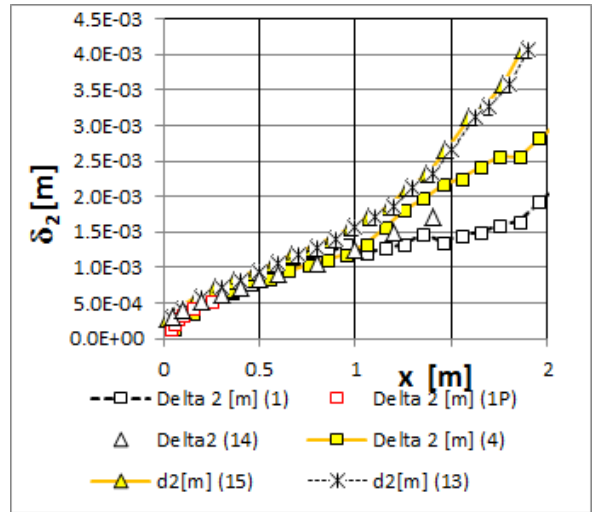


**Figure 6** The momentum thickness  $\delta_2=f(x)$ ;  $U_e=5$  m/s; B.L.: (1,4,13,14,15)

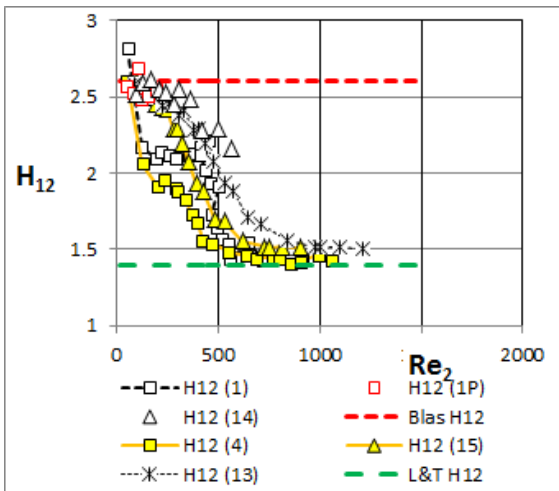


**Figure 5** The shape factor  $H_{12}=f(Re_2)$ ;  $U_e=5$  m/s; B.L.: (1,4,13,14,15),  $H_{12Bl}$ ,  $H_{12LT}$

All above graphs clearly show the effect of leading edge on the transition process. The thin leading edge postponed the start of transition.

Following graphs show developments of the momentum thickness, the skin friction coefficient and the shape factor along the coordinate  $x$ .

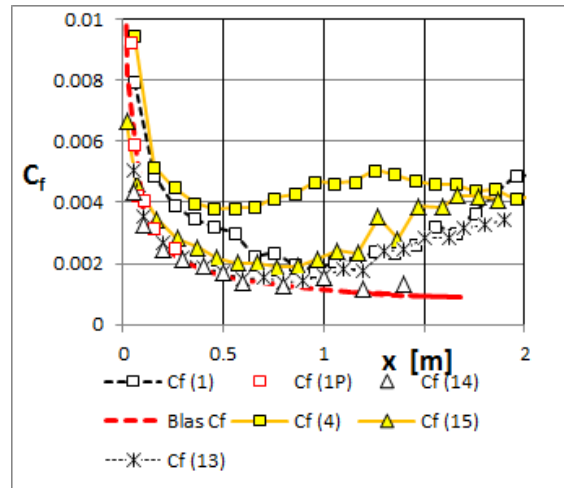


**Figure 7** The skin friction coefficient  $C_f=f(x)$ ;  $U_e=5$  m/s; B.L.: (1,4,13,14,15),  $C_{fBl}$

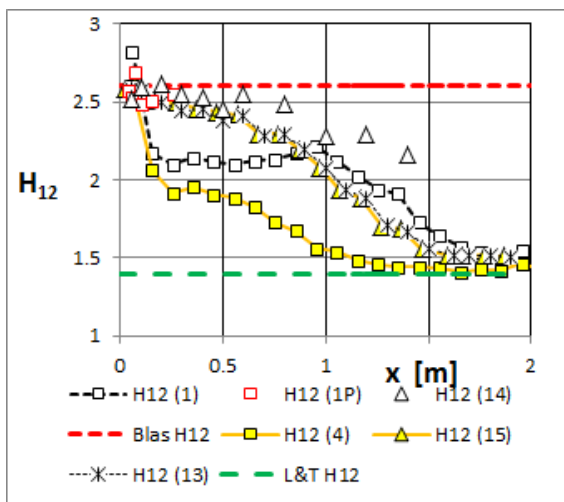


**Figure 8** The shape factor  $H_{12}=f(x)$ ;  $U_e=5$  m/s; B.L.: (1,4,13,14,15),  $H_{12Bl}$ ,  $H_{12LT}$

The comparison of different  $U_e$  should show the effect of Reynolds number on transition process. Neither the skin friction coefficients  $C_f$  (1-3) in case of natural turbulence (fig. 9), nor the coefficients  $C_f$  (4-6) in case of grid turbulence (fig. 10), show any remarkable differences.

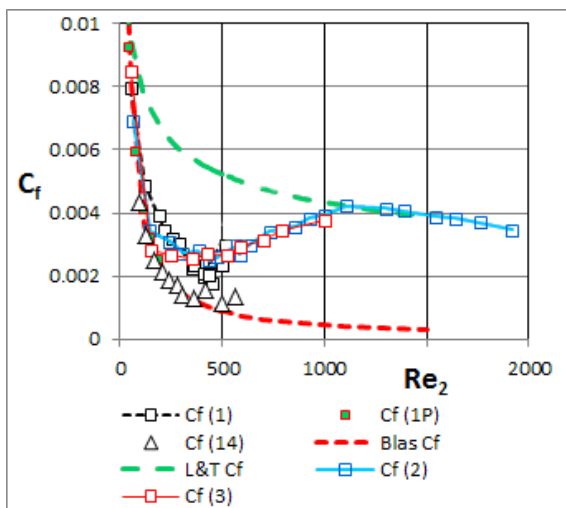


**Figure 9** The skin friction coefficient  $C_f=f(Re_2)$ ; natural turbulence  $Iu_e=0.3\%$ ; B.L.: (1,2,3,14),  $C_{fBl}$ ,  $C_{fLT}$

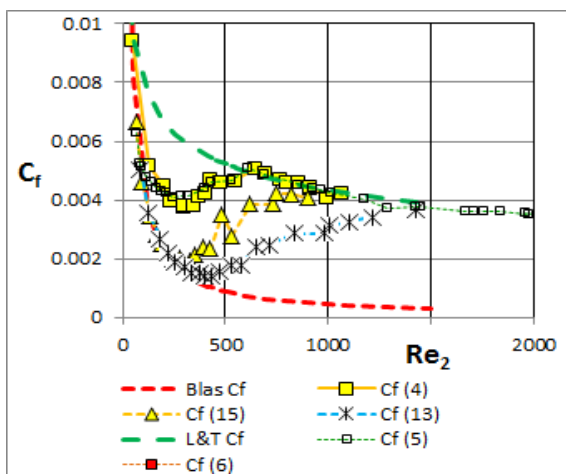


**Figure 10** The skin friction coefficient  $C_f=f(Re_2)$ ; grid turbulence  $Iu_e=3\%$ ; B.L.: (4,5,6,13,15),  $C_{fBl}$ ,  $C_{fLT}$

The shape factors, as well as skin friction coefficients, show that the development is independent from the free stream velocity.

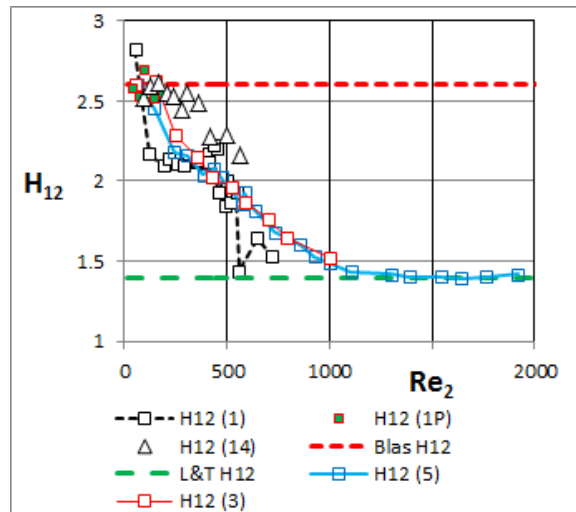


**Figure 11** The shape factor  $H_{12}=f(Re_2)$ ; B.L.: (1,3,5,14),  $H_{12Bl}$ ,  $H_{12LT}$

On the graph in fig. 10, the mentioned effect of leading edge is clearly visible. The transition starts sooner with the MSE6 leading edge (see  $C_f$  4-6) than with the K1 leading edge (see  $C_f$  13, 15). The influence of the shape of leading edge is studied e.g. in [5].

## CONCLUSION

Experimental study of the transition on the smooth flat plate has been done. The turbulence of external flow was either natural or generated by grid. The free stream velocity was set to 5, 10 and 14 m/s. In current experimental setup within the investigated range the effect of the free stream Reynolds number was not observed. The effect of leading edge on the transition process was demonstrated. The well shaped thin leading edge postpones the start of transition significantly.

## REFERENCES

- [1] P. Jonáš, O. Mazur and V. Uruba, On the receptivity of the by-pass transition to the length scale of the outer stream turbulence. Eur. J. Mech. B – Fluids 19, 707-722. (2000)
- [2] O. Hladík, P. Jonáš, O. Mazur, V. Uruba: By-pass transition of flat plate boundary layers on the surfaces near the limit of admissible roughness, EFM 2010. (2010)
- [3] P. Jonáš, ZAMM Z. angew. Math. Mech. 77, S1, pp. 145-146. (1997)
- [4] L.-U. Schrader, L. Brandt, C. Mavriplis, D. S. Henningson, Receptivity to free-stream vorticity of flow past a flat plate with elliptic leading edge, J. Fluid Mech. Vol. 653, pp. 245–271. (2010)
- [5] M. V. Ustinov, A.A. Uspensky, Influence of turbulence skále and shape of leading edge on FST-induced laminar-turbulent transition. Proc. 28th Int. Cong. of the Aeronautical Sciences, pp. 1–10. (2012)
- [6] A.A. Townsend, The structure of turbulent shear flow, Cambridge University Press. (1956)
- [7] J.C. Rotta, Turbulent boundary layers in incompressible flow. Progress in Aeronautical Sciences, Vol. 2, Oxford. (1962)

## ACKNOWLEDGEMENT

This work has been supported by the Grant Agency of the Czech Republic GACR GAP101/12/127. Support is gratefully acknowledged.